Contents lists available at ScienceDirect

HardwareX

The K2: Open-source simultaneous triple-color TIRF microscope for live-cell and single-molecule imaging

Christian Niederauer, Marco Seynen, Jan Zomerdijk, Marko Kamp, Kristina A. Ganzinger *

AMOLF, Amsterdam, The Netherlands

ARTICLE INFO

ABSTRACT

Imaging the dynamics and interactions of biomolecules at the single-molecule level in live cells and reconstituted systems has generated unprecedented knowledge about the biomolecular processes underlying many cellular functions. To achieve the speed and sensitivity needed to detect and follow individual molecules, these experiments typically require custom-built microscopes or custom modifications of commercial systems. The costs of such single-molecule microscopes, their technical complexity and the lack of open-source documentation on how to build custom setups therefore limit the accessibility of single-molecule imaging techniques. To advance the adaptation of dynamic single-molecule imaging by a wider community, we present the "K2": an open-source, simultaneous triple-color total internal reflection fluorescence (TIRF) microscope specifically designed for live-cell and single-molecule imaging. We explain our design considerations and provide step-by-step building instructions, parts list and full CAD models. The modular design of this TIRF microscope allows users to customize it to their scientific and financial needs, or to re-use parts of our design to improve the capabilities of their existing setups without necessarily having to build a full copy of the K2 microscope.
© 2023 The Author(s). Published by Elsevier Ltd. This is an open access article under the CC BY-NC-ND license (http://creativecommons.org/licenses/by-nc-nd/4.0/).

Specifications table:

Hardware name	Simultaneous multicolor large field-of-view total internal reflection fluorescence microscope
Subject area	Single-molecule Biophysics, Fluorescence Microscopy
Hardware type	Total Internal Reflection Fluorescence Microscope
Closest commercial analog	openFrame (Cairn Research), Nanoimager (ONI)
Open source license	CC-BY-NC-ND 4.0
Cost of hardware	100,000€ (excluding VAT)
Source file repository	Design files and data are available at 10.5281/zenodo.7380380.
	A ready-to-view model is available at https://autode.sk/3vdsOu0.
	Data analysis code is available at github.com/GanzingerLab.
	Up-to-date information about the setup is available at the K2 TIRF Github page. (ganzingerlab.github.io/K2TIRF/K2TIRF/index.html).

* Corresponding author.
 E-mail address: ganzinger@amolf.nl (K.A. Ganzinger).

1. Hardware in context

Commercially available fluorescence microscopes for state-of-the-art single-molecule and super-resolution microscopy are often expensive to acquire and lack the flexibility to incorporate custom features beyond already available add-ons. In recent years, a number of open-source projects originated within the super-resolution fluorescence microscopy community, facilitating the design and construction of custom microscopes from the bottom-up [1–7]. Additionally, stand-alone solutions for various sub-components of single-molecule microscopes have been published as open source hardware projects (*e.g.* focus stabilization [8–10], laser sources [11–14], objective heaters [15,16] and beam-shaping devices [12,17–19]). Our microscope design builds on previous open-source projects and our in-house engineering expertise, to provide a cost-effective and flexible solution for single-molecule fluorescence microscopy.

Here, we present a single-molecule total internal reflection fluorescence (TIRF) microscope that is capable of acquiring dynamic single-molecule data with four-color excitation and simultaneous triple-color detection. The microscope uses a single sCMOS camera and projects the fluorescence emission coming from the sample onto different camera regions for each fluorescence channel. Together with homogeneous illumination from a beamshaping device, this enables simultaneous three-color imaging with large fields of view (73μm × 73μm) for each channel. The microscope further features objective heating, a plexiglass cover with an integrated LED array for brightfield illumination, and motorized switching of the angle of the excitation laser beam from TIRF to highly inclined and laminated optical sheet (HILO) and epifluorescence. Finally, the microscope also includes a flip-in lens for fluorescence recovery after photobleaching (FRAP) experiments and a focus stabilization system to correct axial sample drift in timelapse and multi-position measurements.

To ensure reliability and reproducibility of experiments, all imaging settings (*e.g.* laser power, exposure time, stage position, angle of incidence, . . .) are carefully documented for every dataset and saved as *.txt* metadata files. We also monitor and record environmental parameters (temperature, humidity) and the axial sample drift when using the focus stabilization system. This allows us to precisely control and replicate our experiments under identical imaging conditions, which is essential for generating comparable and reproducible data with TIRF microscopes [20].

2. Hardware description

The K2 single-molecule TIRF microscope is comprised of a central cube with the sample stage, sample holder and objective (see Fig. 1 and panel I in Fig. 2), as well as two enclosed boxes. The box on the right-hand side of the central cube houses the excitation path optics and the qgFocus parts (see Fig. 1 and panel II and III in Fig. 2). The box to the left contains the detection pathway, where emitted fluorescence light from the sample is split in up to three spectrally separated channels (see Fig. 1 and panel IV in Fig. 2). The excitation and detection pathways are enclosed in light-tight aluminum boxes to reduce background light levels, minimize laser safety issues, and prevent dust buildup. The entire setup is mounted on a vibration-damped optical table, with additional components (*e.g.* commercial multi-laser fiber-coupled source, panel V in Fig. 2) and the setup control computer located nearby.

2.1. Microscope body

The K2 single-molecule TIRF microscope is a custom-designed instrument that does not use a conventional microscope body (see Fig. 3). The central part is a solid, CNC-milled aluminum block, based on the miCube project [3]. The cube houses
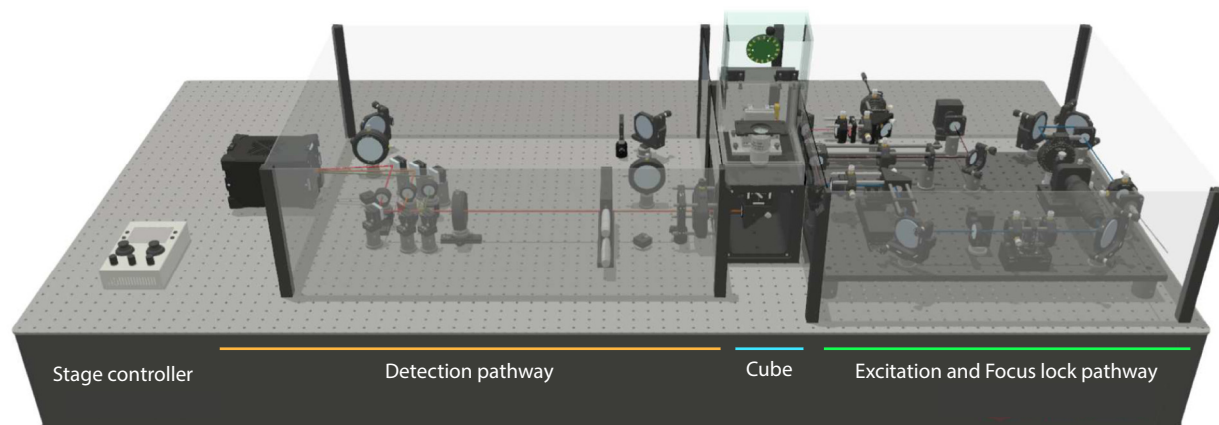

Fig. 1. Render of the K2 open-source simultaneous triple-color TIRF microscope for live-cell and single-molecule imaging. For illustration purposes, the two enclosure boxes to the left and right of the central cube are rendered transparent and their lids are removed. The handheld sample stage joystick controller is placed on the optical bench only for illustration purposes and usually located on the computer desk.
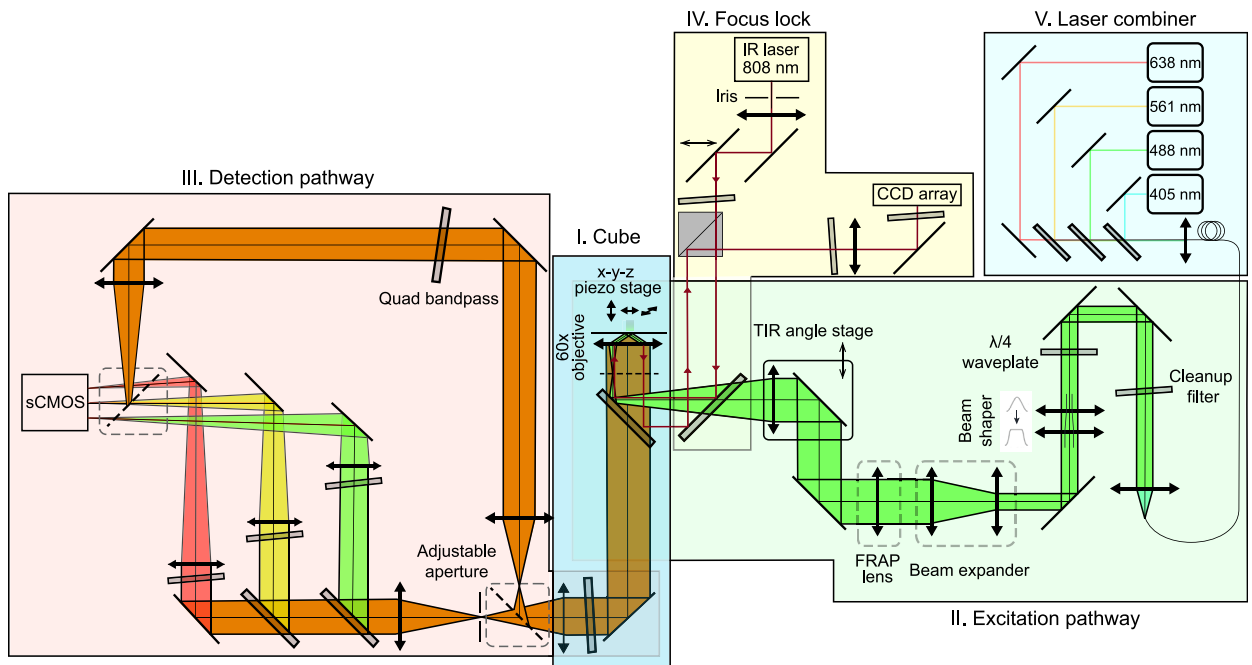
Fig. 2. Optical pathway of the K2 microscope: I) The central cube houses the sample stage, objective, dichroic mirror for splitting excitation and emission light, and the tube lens. II) The excitation pathway launches a four-color laser beam with circular polarization and flat-top beam shape into the central cube. The angle of incidence is controlled using a motorized stage to switch between epifluorescence, HILO- and TIRF-imaging. A flip-in lens can be used to focus the beam at the sample plane for bleaching experiments. III) The detection pathway features a triple-color image splitter, projecting the field-of-view onto different regions of the sCMOS camera chip for simultaneous triple-color imaging. Two mirrors on magnetic mounts can be used to bypass the triple-color image splitter. IV) The focus stabilization pathway uses an infrared laser to detect and compensate for axial drift of the sample. V) A commercial multi-laser fiber-coupled source delivers the excitation laser beam via a single-mode fiber to the setup.

the objective, sample stage, dichroic mirror and tube lens. Unlike traditional commercial microscopes, the K2 does not include an objective turret or ocular, as they are not required for our experiments. This design results in a smaller footprint and excellent mechanical stability.

A high numerical aperture oil-immersion objective (NA = 1.49, CFI Apochromat TIRF, Nikon) with 60x magnification is mounted on a polyoxymethylene spacer to provide thermal isolation from the cube. A polyimide flexible heater, wrapped around the objective with Kapton foil, and a PT100 temperature sensor glued in place, enable precise temperature control via a proportional-integral-derivative (PID) controller (E5CC, Omron). The temper ature data is transferred to the computer via a RS485-to-USB interface. This design is similar to other custom-made and commercial designs [15,16,21], and allows for active heating of the sample, which is thermally coupled to the objective via immersion oil. This enables live-cell imaging and *in vitro experiments at physiological temperatures*.

The sample stage of the K2 single-molecule TIRF microscope is equipped with a three-axis piezo stick–slip positioner (SLS-5252, Smaract) and a two-piece aluminum sample holder that accommodates square (18mm to 26mm side length), circular (25mm to 37mm diameter) and rectangular (62mm to 80mm length, up to 35mm width) samples. Samples are held in place with magnets or an aluminum ring to minimize sample drift. The stage is controlled via the computer or a handheld joystick controller (see Fig. 1) and accurately positions samples with nanometer resolution and 30mm travel range in all directions, allowing for high-throughput measurements of multi-well coverslides.

The excitation laser beam enters the central cube through a port on the right-hand side and is reflected upwards towards the objective by a dichroic mirror. Residual transmitted laser light is absorbed by a neutral density filter mounted on the dichroic mirror cube. Emitted fluorescence collected by the objective is transmitted through the dichroic mirror and reflected via a mirror towards the exit port on the left-hand side of the cube. A four-bandpass emission filter on the mirror mount blocks remaining laser excitation light from reaching the detection pathway. The dichroic mirror and the right-angle mirror are accessible through a door on the front of the cube, which is held in place with magnets.

The central cube is enclosed by a plexiglass cover that protects the sample and objective from dust buildup and improves temperature stability by minimizing convective air transport. A sensor for temperature and humidity is placed inside the plexiglass box and records the environmental parameters during experiments. The lid of the plexiglass cover includes a LED ring for brightfield imaging of cellular targets. For laser safety considerations, potential adopters of our design may consider using a non-transparent cover.
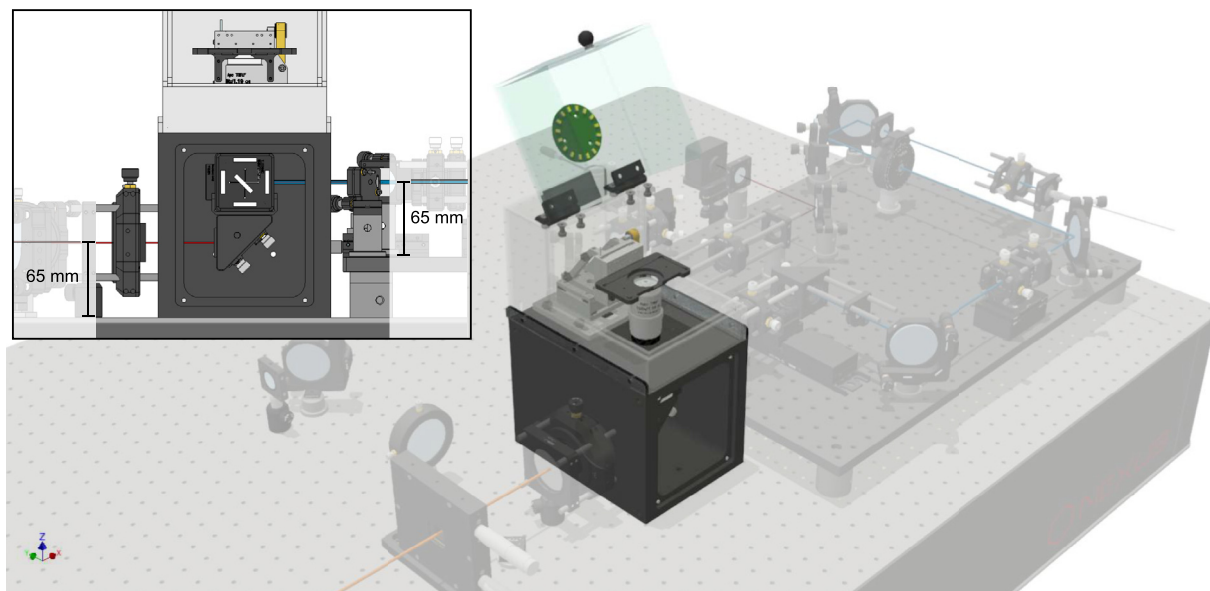
Fig. 3. Central cube of the K2 microscope, showing the TIRF objective mounted on a thermal spacer, the sample stage with sample holder, and the dichroic mirror for splitting emitted fluorescence from excitation laser light inside the cube. The plexiglass cover encloses the objective and sample for added thermal stability and protection, and also provides a brightfield light source. Inset: The placement of the detection port on the central cube determines a beam height of 65mm. The beam height of the excitation path is matched by placing the optical elements on an elevated breadboard, allowing the user to interchange alignment tools and pillar posts between the excitation and detection pathways.

2.2. Excitation pathway

The excitation pathway is mounted on an elevated breadboard (see Fig. 4), which helps to keep the length of posts short for stability. Spacers (39.7mm height) were used to raise the breadboard (12.7mm thickness) to the required level, resulting in final beam heights of 65mm in both the excitation pathway and the detection pathway. In principle, the beam can be brought up to the required height also by using long enough posts or a periscope-assembly.
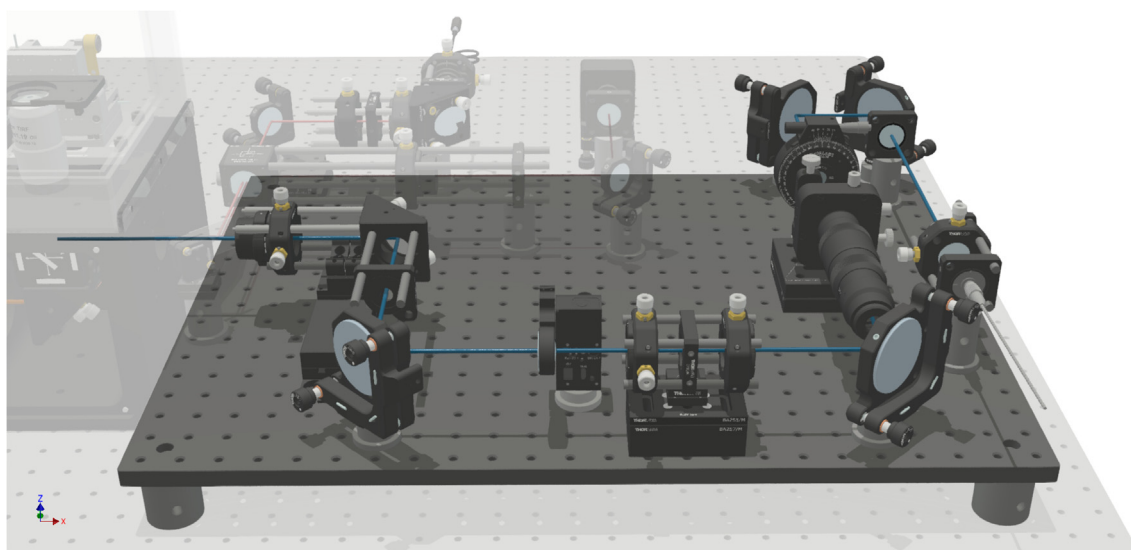

Fig. 4. Excitation pathway of the TIRF microscope, featuring (in the order of placement along the optical path) the fiber collimator, laser clean-up filter, quarter-wavelength waveplate, refractive beamshaper, beam expander, flip-in FRAP lens and motorized stage with TIR focusing lens. These components work together to shape and deliver the excitation laser beam to the sample stage, enabling precise control of the angle of incidence for different imaging modes (*i.e.* epifluorescence, HILO, and TIRF). All parts are mounted on an optical breadboard to match the height of the central cube's excitation port.

We use a commercial multi-laser fiber-coupled source with a single-mode fiber output for delivering four excitation wavelengths (C-FLEX laser combiner, Hübner Photonics; 405nm 140mW, 488nm 200mW, 561nm 220mW, 638nm 195mW) to the excitation pathway. Laser excitation is controlled by a custom-made laser trigger box, that allows alternating and simultaneous excitation synchronized to the camera exposure. Other approaches to laser triggering include the open-source Ries lab laser engine, and the SMILE and NicoLase projects [11,14,22], as well as the commercial Triggerscope [23]. For potential adopters looking to replicate the setup in a more budget-friendly manner, using self-assembled solutions for both laser triggering and laser source could reduce costs by an additional 20 percent [11–14].

The TEM00 laser beam is re-collimated after exiting the fiber to a $1/e^2$ beam diameter of 6mm (@ 561nm), directed through a quad-line bandpass for spectral clean-up, and an achromatic quarter-wavelength waveplate to ensure circular polarisation. The Gaussian laser beam profile is transformed into a flat-top profile using a refractive beam shaping device (piShaper 6_6_VIS, AdlOptica, comparable alternative: TopShape TSM25-10-D-B-6, asphericon) [18,19,17]. A (removable) telescope magnifies the laser beam by a factor of 2.5, resulting in a beam diameter of 15mm. The flat-top profile of the laser beam begins to distort as it propagates over longer distances, so we designed the setup to keep the distance between the beam shaper and the objective as short as possible.

For FRAP experiments, an additional lens on a motorized flip-mount can be inserted into the optical path after the telescope, focusing the excitation laser into a 30µm diameter spot in the imaging plane.

To enable switching between imaging modes (epifluorescence, HILO- and TIRF-imaging, see Fig. 12d), the lens focusing the laser beam onto the back focal plane of the objective is mounted on a motorized stage that allows the beam to be translated off-axis while maintaining its parallel alignment with the objective's optical axis.

The lens that focuses the excitation beam onto the back focal plane of the objective is placed as close to the back focal plane as possible, which allows using a lens with a shorter focal length and therefore a bigger illuminated area at the sample plane. Using a telescope with a higher magnification to achieve an equally-sized illuminated area would result in clipping the laser beam, unless larger optics are used throughout the excitation path. To provide more flexibility in the arrangement of the optical elements, future versions of the central cube could be designed with a reduced distance between the objective port and excitation entry port. With the current design, our setup allows for a maximum homogeneously illuminated diameter of 190µm.

2.3. Detection pathway

The detection pathway is designed under the assumption that the microscope will mostly be used in a triple-color simultaneous imaging mode (see Fig. 5). Using a single camera to capture three color channels simultaneously is more cost-effective than using three separate cameras, and combining a 60x objective without additional magnification with a 2048x2048 px sCMOS chip allows us to achieve large field-of-views (73.65µm × 73.65µm per color channel) nevertheless. To achieve even larger field-of-views, the triple-color detection pathway can be bypassed by placing two mirrors on pre-installed magnetic mounts, resulting in a circular field of view of 190µm diameter. A commercial alternative for image splitting is the OptoSplit (Cairn Research [24]).

As described in the section about the central cube, fluorescence emission from the sample is collected by the objective, passes the quad-bandpass dichroic mirror in the cube and is reflected towards the detection pathway. A quad-line filter blocks residual excitation light from reaching the detection pathway. Emission fluorescence is directed through an infinity-corrected tube lens matching the objective, without further magnification (TTL200-A, Thorlabs). With the camera's physical pixel size of 6.5µm, this results in an effective pixel size of 6.5µm/60 = 108.3nm.

In the triple-color imaging mode, the image of the fluorescent sample is cropped horizontally by a custom razorblade slit aperture in an intermediate image plane. This is necessary to avoid overlapping of the color channels when imaging them
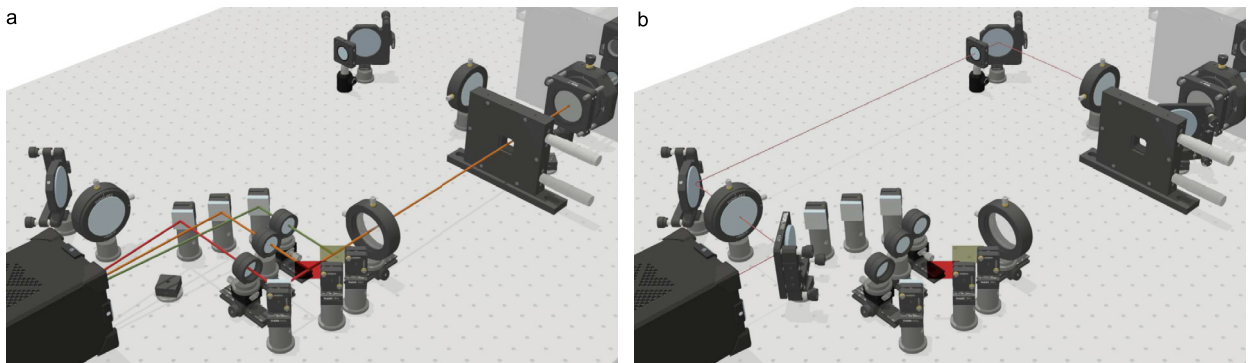

Fig. 5. Detection pathway options of the K2 TIRF. **Left:** triple-color detection pathway with adjustable slit aperture and image splitter for simultaneous imaging of up to three color channels. **Right:** single-color full field-of-view path.

side-by-side on the camera chip (see Fig. S29). Splitting the fluorescence emission into the different spectral channels and filtering them is done in infinity space in a 4f-configuration. This reduces aberrations and allows more mechanical freedom, since the distance of the second to the first 4f-lens is not critical.

The first 4f-lens is positioned to have its focal plane aligned with the image plane formed by the tube lens. Then, the fluorescence emission is split into three colors by two low-pass dichroic mirrors, matched to the four-bandpass dichroic mirror in the cube, and one dielectric mirror. Furthermore, appropriate bandpass filters are placed in each color channel. Individual lenses mounted on rails and dovetail stages project the images of each color channel next to each other on the camera. The use of individual lenses allows precise co-alignment of the image planes and the correction of residual chromatic aberrations. A dielectric mirror is used in each color channel to project the spectrally-separated images onto the camera chip. Finally, three equally-sized square field-of-views are created by cropping the camera chip horizontally. By cropping in line with the scanning of the sCMOS chip, we are able to reduce the read-out time from 22.6ms (full chip, 2048x2048) to 7.6ms (central region, 2048x682). At a typical framerate of 25 fps, this approximately doubles the exposure time per frame (32.4ms/17.1ms $\approx$ 1.89).

The optical path for the image splitter was designed to be as compact as possible to minimize vignetting, while at the same time allowing component accessibility for alignment. Additionally, projecting the image onto the camera at an angle introduces aberrations, therefore the individual focusing lenses and the mirrors are placed as close to each other as possible. As a consequence, this maximizes the distance between the last mirror and the camera and hence decreases the angles at which images are projected from the left and right color channel.

In the single-color imaging mode, the full 190µm diameter illuminated field-of-view is imaged with spatially unseparated color channels. This is accomplished by bypassing the slit aperture and the image splitting pathway using two mirrors, that are placed manually on magnetic mounts. The first mirror is placed after the tube lens and the second mirror before the camera. Two lenses relay the image in a 4f-system, which conveniently also allows the placement of additional components like filters or phase masks in the fourier plane (see Fig. 5, Fig. S28).

2.4. Focus stabilization pathway

In microscopy in general, but specifically in super-resolution and single-molecule experiments and timelapses, sample drift can significantly degrade the quality of the recorded data [25]. In live-cell and single-molecule tracking experiments, lateral drift of the sample usually does not interfere with the experiments as the typical drifting appears on much slower timescales than the molecular movement apparent in the sample (lateral sample drift in our setup: $\approx$ 1nm min^{-1}, diffusion of individual receptor proteins in cell membranes: $\approx$ 0.1µm^{2}s^{-1} to 1µm^{2}s^{-1}) [26–29].

Movement of the sample along the optical axis (axial drift), however, leads to a shift of the focal plane. Since in TIRF microscopy, fluorescence is only emitted from a thin layer close to the coverslip, this shift leads to a decreased signal-to-background ratio due to the defocus blurring of the point spread function, or even the loss of the object that the user initially focused on. Therefore, keeping the sample in focus is crucial, especially when performing hour-long measurements and timelapses, or repeated acquisitions on different areas on a sample.

One way to measure and control the distance of the sample from the objective is to use the back-reflection of the excitation laser, with the drawback that measuring and updating the z-position can only be done during the excitation cycle [8]. A dedicated infrared laser is a more versatile option, as it does not excite commonly used fluorescent proteins and dyes, allowing for continuous measurement and control of the sample's axial position without interfering with fluorescence measurements.

The principle of the focus stabilization is depicted in Fig. 6a. First, the sample is brought into focus manually and the position of the back-reflected beam is stored. Axial drift Δz of the sample leads to a lateral displacement Δd of the totally internally reflected infrared laser beam. The back-reflected laser beam is relayed through additional optics, resulting in a displacement $\Delta d\prime$, that is determined by comparing the center peaks of the previously saved reference and the currently measured laser profiles on a line-array sensor. To mechanically compensate for the axial drift, an active control mechanism reacts to the lateral displacement and moves the sample stage to keep the position of the back-reflected beam stable.

Our focus stabilization implementation (see Fig. 6b), qgFocus (short for **q**uite **g**ood Focus), is similar to other custom-built and commercial designs such as pgFocus [10] or CRISP [9]: A collimated infrared laser is coupled into the excitation path by a short pass dichroic mirror and attenuated with a neutral density filter so that it does not interfere with the fluorescence signals. A manual micrometer stage is used to shift the infrared laser beam off-axis, bringing it into total internal reflection. The infrared laser is then focused at the back focal plane, reflected at the glass-sample interface, and travels back towards a beamsplitter. The back-reflected laser beam is diverted by the beamsplitter towards a bandpass filter and finally focused onto a linescan sensor (TSL1401, Parallax). The signal is read-out and time-averaged internally, before it is sent to the computer (the update rate is adjustable, typically used rates are 10-30Hz). A Gaussian function is fit to the intensity curve, and a control loop that locks onto the saved in-focus position of the Gaussian function center then moves the piezo-driven sample stage in the axial direction to maintain focus. In our system, manual sample travel in x-y during focus-controlled experiments is limited to 100µm s^{-1} to avoid jumps in the back-reflected beam position that cannot be followed by the control loop.
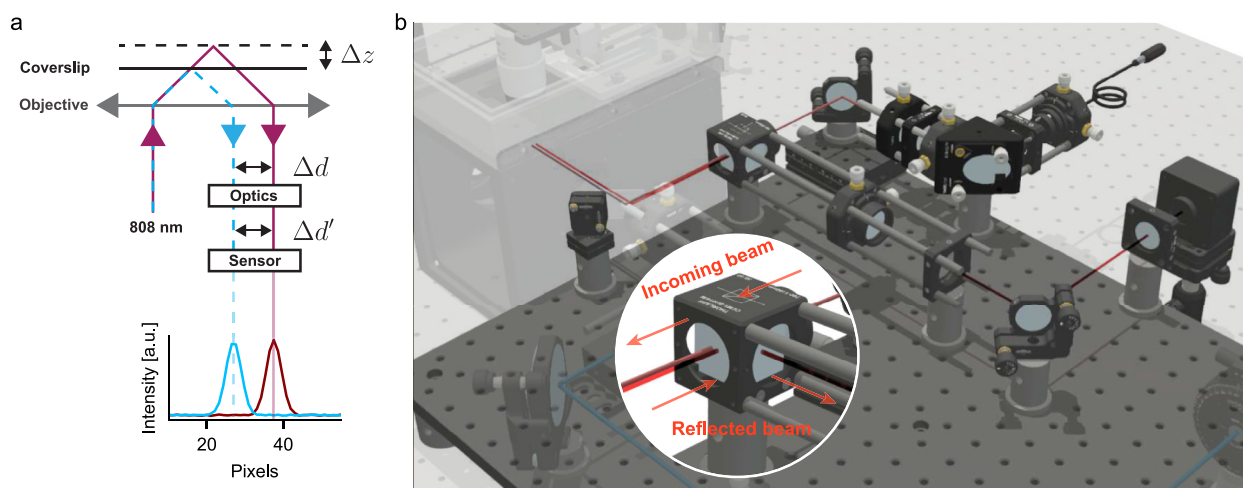
Fig. 6. a) Schematic of the qgFocus focus stabilization: an infrared laser beam is focused off-center at the back focal plane of the objective and is totally internally reflected at a coverslip. Upon an axial movement Δz of the coverslip, the reflection of the beam is shifted laterally by a distance Δd, which is translated into a distance $\Delta d\prime$ through downstream optics. A sensor registers the intensity profile of the back reflected beam and determines its center by a Gaussian fit. A control loop acting on the sample stage moves the sample such that the displacement of the currently measured intensity profile and of the referenced intensity profile is approaching zero. **b**) Render of the focus stabilization pathway of the K2 TIRF, mounted alongside the excitation optics on an elevated breadboard. Inset: Separation of incoming infrared laser beam and back-reflected beam by a beamsplitter cube.

2.4.1. Scripts

Our microscope control software includes a script interface that allows users to control the setup and perform various tasks using C# commands. Examples of scripts that can be run using the interface are available at github.com/Ganzinger-Lab/K2TIRF/tree/master/K2TIRF/scripts. The available examples include a simple *x-y* raster scanning script, a laser power calibration method that we used to calibrate the laser percentage settings (see Fig. S50) and a script that continuously moves the sample stage up and down, which we used during the alignment process (see Fig. S26 and Fig. SM1).

3. Design files

A complete CAD assembly of the setup with all optical components has been uploaded to the public repository Zenodo (10.5281/zenodo.7380380). Please note that while we tried to reproduce the physical positions and distances of the optical components as faithfully as possible, this CAD model mainly serves illustration purposes and should not be used as an alignment guide.

For all custom-made mechanical components, CAD files and technical drawings are provided, following best practices for sharing reproducible microscope hardware [30]. For all custom-made electronic components, PCB layouts and electronic design files are provided. A ready-to-view CAD model is uploaded to Autodesk Drive (https://autode.sk/3vdsOu0). The source code of the software for the operation of the setup is uploaded to the Zenodo repository. Python code for processing and analyzing single-molecule imaging data is available at the Ganzinger group Github (github.com/GanzingerLab).

Description	File type	License	Location of the file
Virtual K2 setup	CAD model	cc-BY-SA-4.0	10.5281/zenodo.7380380
Central cube	Technical drawing	cc-BY-SA-4.0	10.5281/zenodo.7380380
Sample holder	Technical drawing	cc-BY-SA-4.0	10.5281/zenodo.7380380
Thermal spacer	Technical drawing	cc-BY-SA-4.0	10.5281/zenodo.7380380
Plexiglass cover	Technical drawing	cc-BY-SA-4.0	10.5281/zenodo.7380380
Cage assembly adapter plate	Technical drawing	cc-BY-SA-4.0	10.5281/zenodo.7380380
Adjustable slit aperture	Technical drawing	cc-BY-SA-4.0	10.5281/zenodo.7380380
Gustafsson alignment tool	Technical drawing	cc-BY-SA-4.0	10.5281/zenodo.7380380
qgFocus unit	Technical drawing, Electronical circuit design, PCB layout	cc-BY-SA-4.0	10.5281/zenodo.7380380
Trigger box	Electronical circuit design	cc-BY-SA-4.0	10.5281/zenodo.7380380

4. Bill of materials

The up-to-date bill of materials for the K2 TIRF project is available on the open-access Github page (ganzingerlab.github.io/K2TIRF/K2TIRF/component_table.html), providing detailed information on the components and materials needed to build the microscope.

5. Build instructions

For an overview of the layout of the optical components, see Fig. 1 (CAD-model render), Fig. 2 (schematic of the optical pathway) and Fig. 7 (picture of the setup). The setup requires approximately 190cm by 90cm of optical bench space, as well as a similar area (*e.g.* above the optical bench) for the laser combiner, objective heating PID controller and laser trigger box, as well as space for the computer and screens.

When setting up the microscope, the most convenient approach is to start with building and aligning the excitation pathway and use the laser source for alignment. However, if this step needs to be deferred and another laser source is available (*f. i.* the Gustafsson alignment tool), it is possible to begin with the central cube and the detection pathway, since the excitation and detection pathways can largely be assembled and aligned independently of each other. In addition to commonly used alignment tools such as viewing disks, reticles, irises, and calibration slides, we use a cage system mounted on the objective port to simplify the alignment of the excitation path, and the Gustafsson alignment tool for the detection path alignment [31]. The Gustafsson alignment tool is a small diode laser aligned in a mount that is screwed into the objective thread. The wavelength should be situated within one of the fluorescence emission bands, *e.g.* in the GFP-like emission band between 500nm and 550nm. This allows the alignment laser to pass through the emission dichroic mirror, and, if alignment is performed in the correct order, the laser beam can be used to align the entire detection pathway. General approaches and recommendations for the alignment of optical parts are described in [32].

Detailed, step-by-step build instructions are provided in the supplementary information.

6. Operation instructions

To ensure optimal performance and data quality of the setup, it is important to verify the multicolor-channel alignment of the microscope regularly and update the correction map, as described in Fig. 11. Furthermore, drift in the alignment of the excitation path can be checked by confirming the stage positions at which the laser beam is in epifluorescence and entering the TIRF regimen. Additionally, it is essential to check the laser powers with a power meter to ensure they are within the specified range. Dust specks on optical surfaces can interfere with imaging, therefore it is recommended to carefully remove
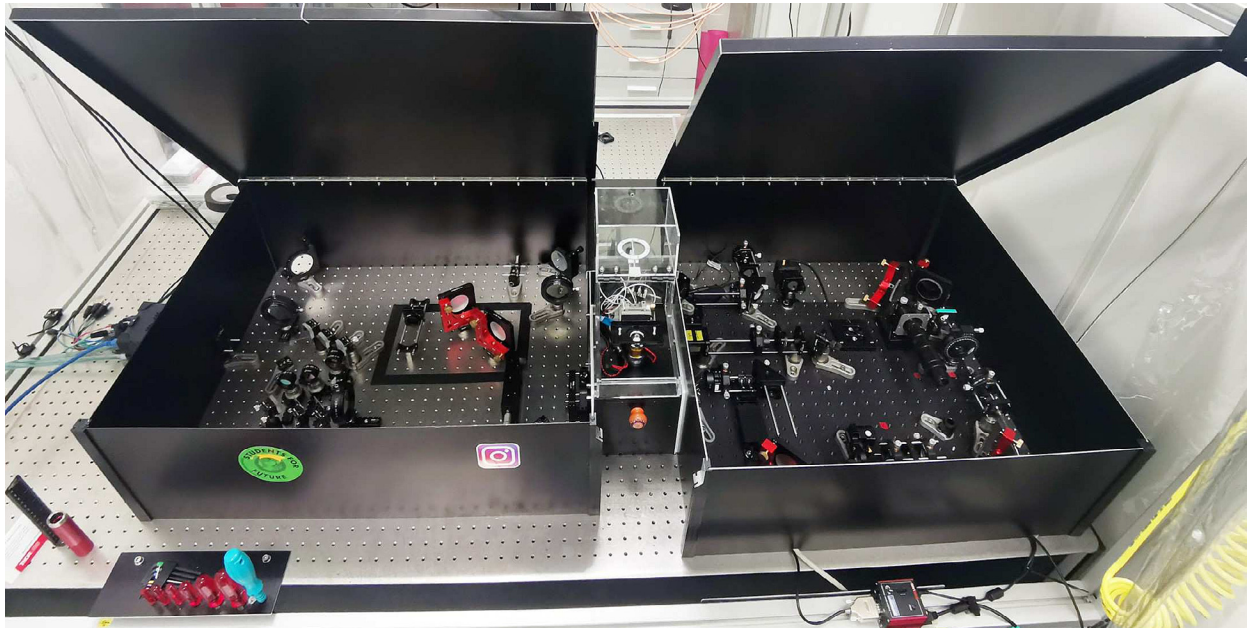

Fig. 7. Picture of the K2 TIRF microscope. From right to left, there are the excitation and focus stabilization pathways on an elevated breadboard, the central cube with the objective, sample stage and a plexiglass cover, and the triple- and single-color detection pathways with the camera on the left. The excitation and detection pathways are enclosed in light-tight aluminium boxes to reduce background light levels, minimize laser safety issues, and to prevent dust from building up.

dust specks using oil-free air or nitrogen gas on the particular element. Any spilled immersion oil should immediately be removed with lint-free wipes and the contaminated surfaces cleaned with Ethanol. By following these guidelines, the microscope can be kept in optimal working condition, resulting in reliable and high-quality data.

6.1. K2 software

A software package for operating the setup was written in C#. It features a graphical user interface (GUI) that provides a simple and intuitive way to control and customize the microscope setup for different experiments. The GUI includes a number of panels for changing settings and directly controlling the various components of the microscope, such as the camera, stage, lasers, and qgFocus. Fig. 8 and Fig. 9 show some of the most important panels for controlling these components. The software also allows users to save experiment routines as templates, with a wide range of custom settings and options. The source code has been uploaded to the public repository Zenodo (10.5281/zenodo.7380380), excluding any third party software and internal libraries which are shared among other projects in the institute. Thus, this release will not compile into the final product but it can serve as an inspiration for other development efforts. For all commercial components (stage, camera, lasers, flip-in lens, TIR angle stage) LabView virtual instruments, python libraries, and/or micromanager plugins [33] exist and can be used alternatively for the setup control (see Fig. 10).

In the following, the operation of the setup is described using the K2 software.

6.1.1. Camera

The camera panel (Fig. 8a) provides access to all relevant camera settings, such as the exposure time, region of interest, pixel binning, and bit-depth. The Start/Stop buttons can be used to activate or stop the camera live-view streaming (Fig. 15), and the Snap button takes a single frame snapshot.

6.1.2. Live-view and RGB viewing mode

The camera image is streamed in the live-view mode, allowing the user to position the sample and to search for a suitable region of interest, as well as to determine appropriate imaging conditions, such as laser power and exposure time. The contrast and colormap settings of the streamed image are set by the user (Fig. S46). The K2 software also features a RGB viewing mode, that superpositions the triple-color separated camera channels as a red-green–blue overlay in the live-view (Fig. S47). This allows to quickly assess colocalization in different channels and therefore speeds up screening for an interesting cell or region of interest on the sample, and is a convenient tool during the alignment of the triple-color image splitter (see Fig. S26).
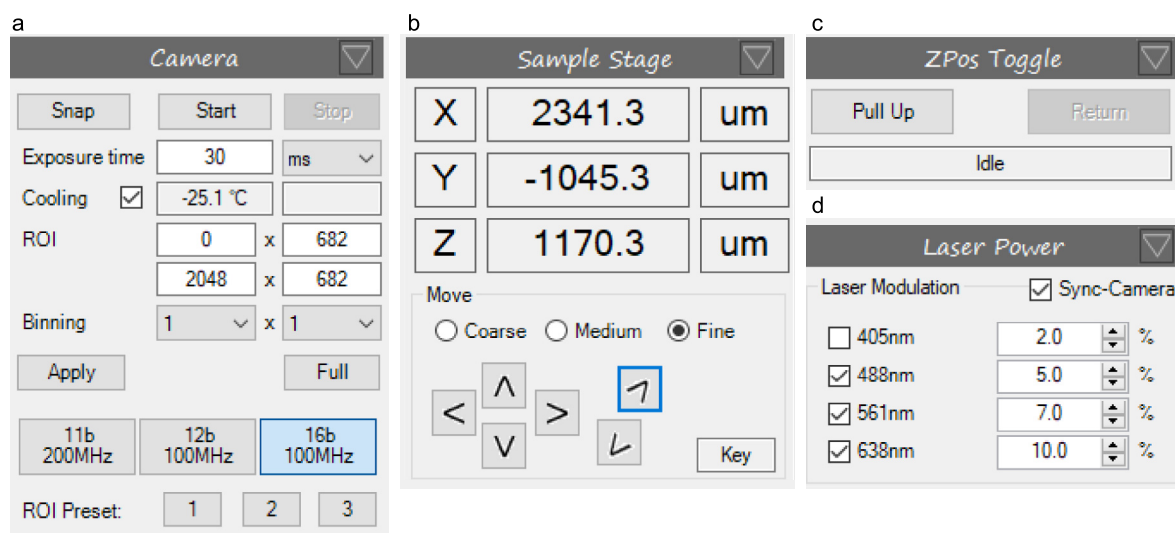

Fig. 8. Main control panels of the K2 software: **a**) Camera: In this panel, the exposure time, manual/preset regions of interest (*ROI*), binning and bit-depth of the camera are configured, as well as live-viewing of the camera image (Start/Stop) and snapping a single frame (Snap). **b**) Sample Stage: Piezo stage position readings, and arrow keys (operated via cursor click or with arrow keys on keyboard), complementary to the physical joystick, with three user-defined step sizes. **c**) Zpos Toggle: Toggle for pulling up the sample away from the objective, and returning the sample to the initial *z* position (*Pull Up*, *Return*). **d**) Laser powers: Laser power settings used during camera live-view, calibrated to achieve a linear percent-to-power relation. The synchronization of the lasers to the camera trigger can be switched off.
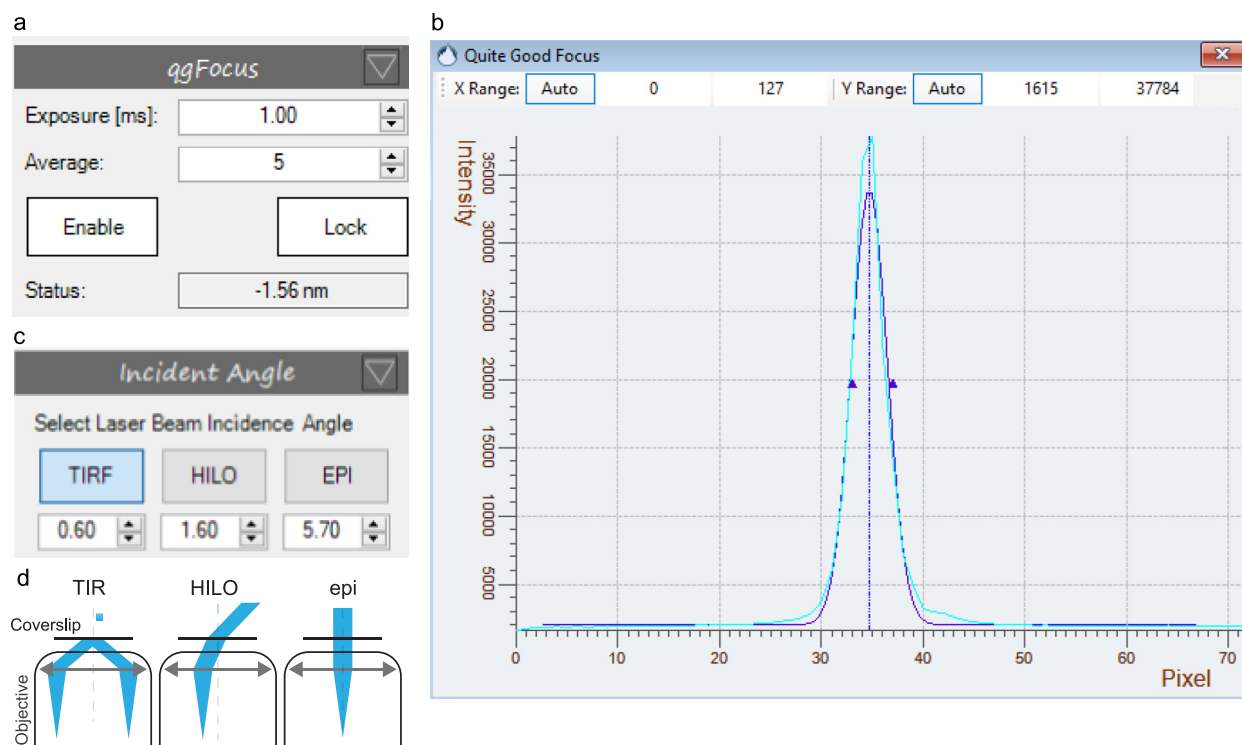
Fig. 9. a) qgFocus control panel to switch on the focus stabilization sensor (*Enable*), to engage the focus stabilization (*Lock*) and to set the exposure time and number of averaging cycles. The *Status* reports on the current distance of the stage with respect to its initial *z*-position. **b)** qgFocus sensor output displaying the measured back-reflected laser intensity profile on qgFocus sensor (cyan line) and a Gaussian fit to the intensity profile (blue line). **c-d)** TIR stage panel: Stage positions for TIRF, HILO and epifluorescence imaging are set and can be called during the experiment to change the angle of incidence of the excitation laser beam.

6.1.3. Sample stage

The piezo stick–slip stage is steered both with the software (either by clicking on the sample stage panel arrows, or using arrow keys on the keyboard) and by a handheld joystick controller. To ensure safe and efficient sample handling, the user can adjust the step sizes *Coarse*, *Medium* and *Fine* and define position limits (Fig. S48).

A *z*-position toggle is available that improves the experimental workflow and reduces the amount of immersion oil needed for high-throughput measurements. It works by moving the sample upwards away from the objective, with *x* and *y* positions unchanged. The sample is first moved slowly (at 0.8mm s^{-1} for 3mm), to avoid introducing air bubbles into the immersion oil and to give the fluid time to draw back to the objective (see Fig. SM2). The sample can then be exchanged or moved horizontally, and returns to the previous *z*-position, again approaching the last millimeters towards the objective slowly. This considerably improves the handling when several samples are imaged and need to be exchanged often. When using multi-well samples, or when imaging many different regions on a single sample, the *z*-position toggle is used for removing the sample from the immersion oil, repositioning in *x-y*, and moving it back to the original *z*-position (see Fig. SM3). This reduces the amount of immersion oil that has to be reapplied and thus allows for high-throughput measurements with minimal user interaction. The exact values for the distance and speed limits are user-defined in the K2 software backend settings (Fig. S49).

6.1.4. Laser powers

The laser powers panel controls laser on/off state and excitation power, and features the option to deselect synchronization of the excitation to the camera exposure. A linear relation between the power percentage set by the user and the actually delivered laser power is established in an initial calibration step (see Fig. S50).

6.1.5. qgFocus

In the qgFocus panel, the focus stabilization sensor's exposure time and number of averaging cycles are set (Fig. 9). Within an axial range of about 5μm around the samples' in-focus position, the back-reflected infrared laser is registered as a sharp peak on the qgFocus sensor and fit with a Gaussian function. For keeping the focus position stable, the center position of the Gaussian fit is saved and used as the setpoint for a control loop.
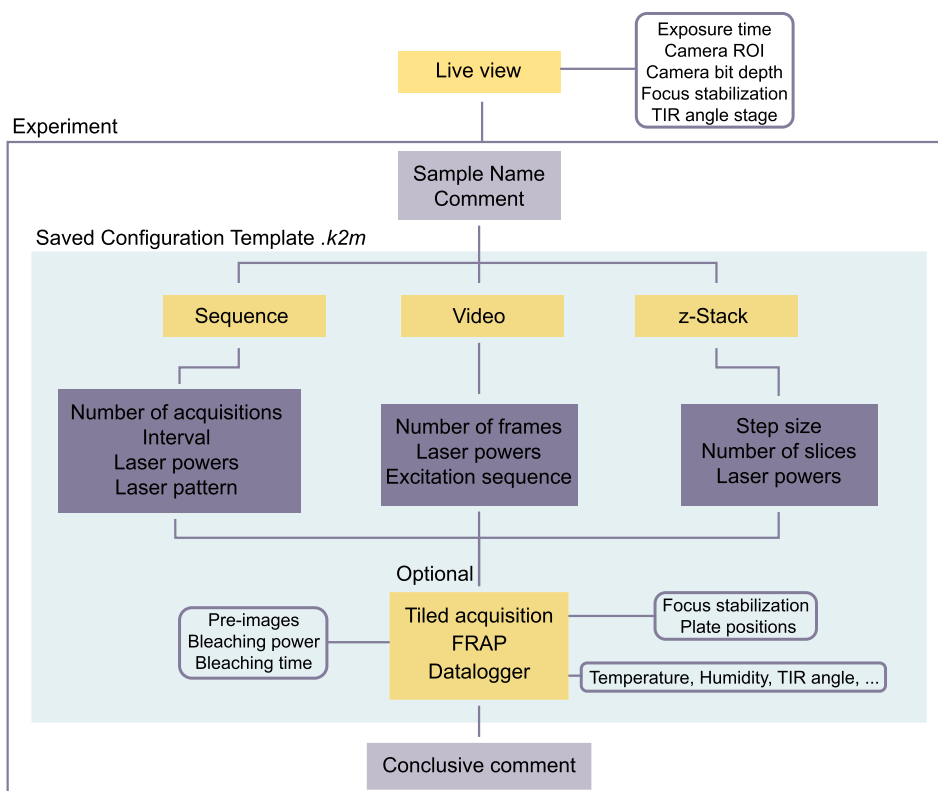
Fig. 10. Experiments configuration diagram: Experimental settings are optimized during live-view. An acquisition is then performed by configuring, or reusing a experiment configuration template and adding details about the sample and experimental conditions. For the acquisition itself, three options (*Sequence*, *Video* and *z-Stack*) are available and for each option, the necessary settings are configured. Optionally, the experiment can be performed at different sample positions (*Tiled acquisition*), as a *FRAP* experiment, and with additional recording of environmental parameters. After the experiment is performed, a comment may be added to the file.

During the initial usage of the setup, determine the control loop variables to ensure that the focus position stabilizes within a few seconds after moving the sample in *x-y* (used values: proportional gain 0.7, integral time 2s, integral limit 1×10^{10}s). Once the qgFocus is engaged, the qgFocus panel displays the extent to which the stage has been shifted to maintain the sample in focus. The sample stage movement is restricted to a speed of $100\mu m\,s^{-1}$ to allow the qgFocus to follow the sample's *z*-position continuously. This speed limit can be defined by the user in the K2 software backend settings (Fig. S51).

6.1.6. Angle of incidence

The motorized TIR stage sets the angle of incidence of the excitation laser beam, allowing the user to switch between epifluorescence, HILO and TIRF imaging modes by calling user-defined positions on the Angle of Incidence panel (see Fig. 9).

When operating the setup the first time, the TIR stage positions corresponding to the different imaging modes are determined with a fluorescent sample (*e.g.* dye in solution) mounted: Starting from the epifluorescence position after setup alignment, the TIR stage is initially moved 4.5mm, and then in steps of 0.1mm. The transition from epifluorescence to TIRF imaging is easy to recognize (see [34] for a detailed description), as interference patterns caused by specs of dust scattering the coherent excitation laser beam, become visible. In sparse single-molecule type of samples, these interference patterns are not visible, but the transition is marked by a sharp increase in the signal-to-background ratio [5]. HILO imaging, where the laser beam penetrates the sample at an angle instead of being totally internally reflected, is typically performed close to the TIR setting (*i.e.* between 4mm to 5mm from the epifluorescence position).

6.2. Pre-configuring experiments

Imaging conditions and sequences may be pre-configured as saveable experiment configuration file (*.k2m*) and can be reused as templates. The user can choose from three general modes: a) Sequence acquisitions, where a pre-programmed laser excitation sequence is looped through every timepoint - for a user-defined number of times, allowing for both alternating laser excitation style experiments and simple timelapses. b) Video acquisitions at the maximum camera framerate,

with one or several lasers simultaneously activated. c) z-stacks, where images are taken at pre-defined axial positions, with one or several lasers switched on.

Each of these modes can be combined with a FRAP experiment at the beginning of the recording, or a tiled acquisition. During a tiled acquisition, the software performs the pre-configured acquisition at different, pre-defined stage positions.

The experiment configuration, sample name and optional comments are saved as a *.txt file along with the microscopy data (*.raw and *.yaml.)

6.2.1. Sequence acquisition

For certain experiments (*e.g.* FRET), fluorophores need to be (alternatingly) excited by a single excitation wavelength at a time. This can be done by performing a Sequence Acquisition (see Fig. S55). Any excitation sequence, with one or several lasers excited during a given camera frame, can be pre-programmed, and is looped through for every timepoint throughout the duration of the experiment. The interval between each timepoint can be set, which also allows for timelapse recordings (see Fig. S56).

6.2.2. Video acquisition

The video acquisition mode allows the simultaneous imaging of multiple color channels, *e.g.* for multi-color single-molecule tracking experiments, at the maximum camera framerate without intervals between acquired frames. For every frame, the same pre-defined set of lasers at a certain power percentage will be used to excite the sample (see Fig. S57). Additionally, there is the option to use in-frame alternating laser excitation. For simultaneous imaging of blue excitable dyes (*e.g.* ATTO488) and cyanine dyes (*e.g.* ATTO643), this was demonstrated to decrease the bleaching of red dyes induced by the 488nm laser drastically [35]. The duration of the pulses is set to be at least ten times smaller than the total frame exposure time, and the triggering scheme is such that the 488nm laser is pulsing anti-cyclic with respect to the others (see Fig. S58).

6.2.3. zStack

Although TIRF microscopy implies collecting fluorescence from the sample surface plane, most TIRF setups allow changing the angle of incidence to HILO or epifluorescence imaging. In these imaging modes, a z-stack can deliver additional information along the axial dimension. The K2 software requires a starting z-position, the number of slices and z-step per slice and will record one frame per slice with a given laser power and exposure time. During the acquisition, the focus stabilization is disengaged and the sample is moved back to the original z-position after the last slice.

6.2.4. FRAP

Fluorescence recovery after photobleaching (FRAP) is a method for studying diffusion dynamics by bleaching the sample locally and observing the recovery of fluorescence by diffusive exchange of unbleached fluorophores into the bleached area. A FRAP experiment in the K2 setup is performed by collecting a number of pre-bleaching frames (either in Sequence- or Video-mode), followed by a bleaching phase where the flip-in lens is flipped into the excitation path, the power of one or several lasers is increased. After the bleaching phase, the recovery is recorded using the Sequence- or Video-mode (see Fig. SM4). Between bleaching and the recovery phase, a short delay is introduced to account for the finite flipping time of the flip-in lens (flip-in: 0.5s, flip-out: 1s). The area and the position of the bleached spot is determined by the positioning and focal length of the flip-in lens.

6.2.5. Tiled acquisition

Coordinates (x, y and z) of stage positions can be generated (*e.g.* for a raster scanning of the sample, see Fig. S52), saved in a list and called manually, or automated during an experiment where a pre-designed (sequence, video, and/or FRAP) acquisition is performed at each position of the coordinate list (see Fig. SM3). If the focus stabilization is engaged, the stored z-position is ignored.

6.3. Starting up the setup

Before turning on the lasers, verify that any removable optical component (beamshaper, beam expander, mirrors for bypassing the triple-color pathway) and filters are placed correctly depending on the experimental requirements. Make sure that the flip-in lens is flipped out, the TIR stage is in a safe position, the objective correction collar is in the correct position, and that the objective was cleaned properly by the last user. If heating is required, make sure to turn it on about 30min before the experiment, to allow the temperature to stabilize (see Fig. 15).

Switch on the required power supplies (lasers, camera, camera cooling, motorized stages and mounts, computer) and mount the sample. Open the setup control software and initialize the motorized stages. Switch on the appropriate lasers at a low power and start the qgFocus and the live-view of the camera. Bring the sample into focus using the sample stage joystick controller. As described before, during the initial operation, the qgFocus control loop settings and the TIR stage positions for epifluorescence, HILO and TIRF imaging should be determined to ensure optimal imaging performance.

7. Validation and characterization

7.1. Multicolor channel alignment

Chromatic dispersion and misalignment of optical elements in the detection pathway lead to distortions across the different color channels, complicating the analysis and interpretation of multicolor microscopy data. Especially for (single-molecule) colocalization experiments, different color channels need to be precisely co-aligned. The physical alignment of the color-splitting optical path is done while imaging a calibration slide and superimposing the three color channels, as described in the supplementary build instructions (see Fig. S26). In doing so, we achieve an average spatial variation across different color channels below 1μm. The remaining spatial offset between the channels is then corrected computationally: first, accumulated bead positions from raster scanning the calibration slide are assigned throughout the corresponding channels (see Fig. 11a-b). A spatial correction map is then calculated (Fig. 11c) using a recently introduced method based on Zernike polynomial gradients [36]. Using this correction map, mean residual spatial variations are below 30nm (Fig. 11c-d).

7.2. Sample drift and focus stabilization

Minimizing sample drift is crucial in (TIRF) microscopy to ensure optimal signal-to-background ratios and the reproducibility of measurements. Therefore, we evaluated the axial and lateral drift of our K2 TIRF microscope, with and without the focus stabilization, during a three hour experiment. Fluorescent beads (TetraSpeck Microspheres, 0.2μm) mounted on
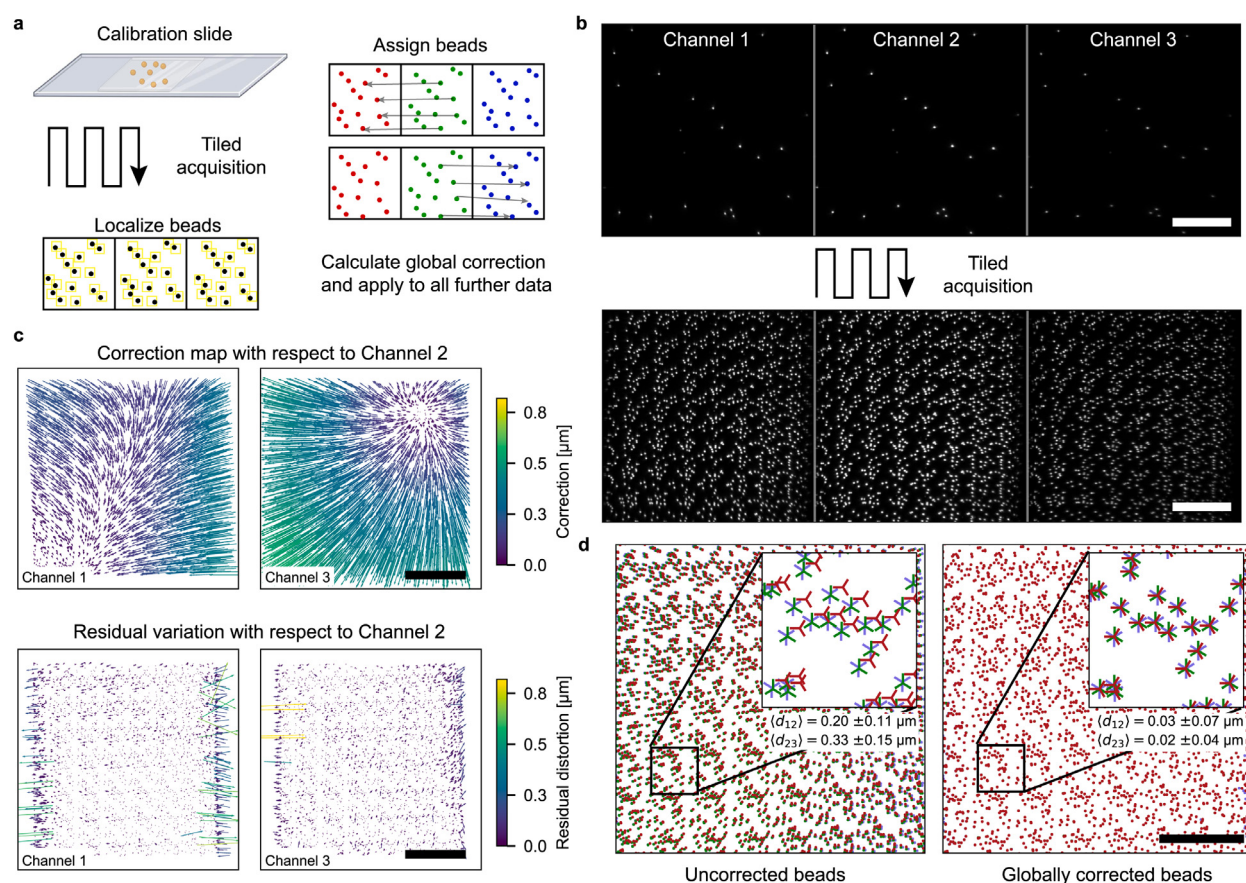

Fig. 11. Multicolor channel alignment a) Multicolor-labeled Tetraspeck beads are deposited sparsely on a coverslide and imaged at multiple positions to collect a large number of $x-y$ sample points. Identical beads are identified in the three color channels and localized frame-by-frame. Variations of bead $x-y$ coordinates relative to the center channel are calculated pairwise, and used to compute a global correction map. This correction map is then used to correct single-molecule localizations acquired in further experiments. **b)** Upper row: Image of Tetraspeck beads in the three color channels, for a given sample position. Lower row: Maximum projection of all bead images acquired during a tile raster-scan. **c)** Upper row: Correction maps of left and right channel, with respect to the middle channel. Lower row: Residual spatial variation remaining after the correction is applied to the calibration data. Arrows indicate the direction of the necessary correction, with their length and color representing the amount of correction needed. **d)** Superimposed $x-y$ positions of Tetraspeck beads with uncorrected coordinates (left) and corrected coordinates (right), with average spatial variations $\langle d_{12}\rangle$ and $\langle d_{23}\rangle$ of identical beads in the left and right channel, with respect to the middle channel. Scale bars are 20μm.
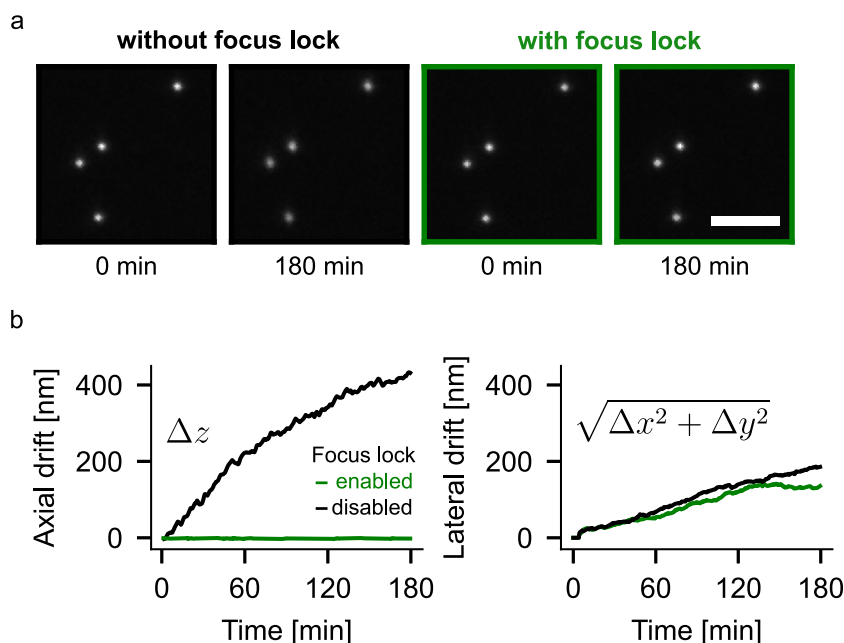
a

Fig. 12. a) Still frames of a sample of fluorescent beads, imaged with and without qgFocus. For the experiment without focus stabilization, there is a slight blurring of beads observable over time, whereas the beads with the focus stabilization enabled stay in focus throughout the entire three hours experiment. For both experiments, the same sample was used, but before each acquisition, the sample was withdrawn from the immersion oil and re-positioned, to avoid biases due to non-identical settling times of the mounted sample. One frame was captured every 30s for three hours. Scale bar is 5μm. **b**) Representative axial and lateral sample drift during a three hour experiment with and without enabled focus stabilization. Left: Axial drift, right: lateral drift of tracked beads, given by the euclidean distance of their current position versus their position in the first frame.

the surface of a microscope slide were used as fiducials. The axial drift during experiments without focus stabilization (Fig. 12a) is observable as a slight blurring of the beads, which is not the case for experiments with enabled focus stabilization. The axial sample drift was quantified by converting the lateral displacement of the back-reflected laser on the sensor into an axial distance. The displacement-to-pixel was determined in an initial calibration experiment (Fig. S51, 1px $\hat{=}$ 561nm). Fig. 12b shows the axial drift throughout the three hour experiment exceeded 400nm without focus stabilization, whereas virtually no residual drift was detectable when the focus stabilization was enabled (mean and standard deviation of the displacement from the in-focus position: -1.74 ± 2.41nm).

Lateral drift was quantified by tracking the fiducial beads and calculating their euclidean distance from their original position at the start of the experiment. We found the lateral drift to be similar with and without focus stabilization enabled, which is expected since the focus stabilization only compensates the axial drift. In comparison to other setups [37–39], the lateral drift is extremely low ($\approx$ 200nm in three hours), which is likely due to using a closed-loop piezo stage not only for the z-axis, but also for x- and y-axes. Most commercial and home-built setups use servomotors for the x- and y-axes, with at least one order of magnitude worse resolution and stability [37,40,41].

7.3. Field-of-view and illumination homogeneity

One of the key features of the K2 TIRF microscope is its large field-of-view that is flat and homogeneously illuminated, which facilitates conducting statistically sound and quantitative single-molecule fluorescence experiments. Using a refractive beamshaper and appropriate optics, we are able to evenly illuminate a large field of view up to 190μm in diameter, providing a high signal-to-background ratio across the entire field of view. This is especially important for dynamic live-cell or single-molecule tracking experiments (*e.g.* cellular activation essays, kinetic studies of molecular interactions), because events may be non-recurrent and capturing as much data from a single field of view as possible with little to no spatial variation in imaging quality is essential (Fig. 13c).

In addition, the large 2048 × 2048 px camera chip allows the imaging up to three color channels simultaneously side-by-side without the need to invest in multiple, synchronized cameras. Simultaneous capture of multi-color emission is important for accurately tracking fast dynamic processes of multiple species of fluorescently labeled molecules in cellular and artificial environments. For triple-color simultaneous imaging, the camera is cropped to produce three equal-sized fields of view of 682 × 682 pixels, or 73.656μm × 73.656μm (see Fig. 13).

Furthermore, the homogeneous illumination of the field of view of the K2 microscope not only provides a high signal-to-background ratio across the entire field of view, but also enables seamless stitching of images acquired by raster-scanning
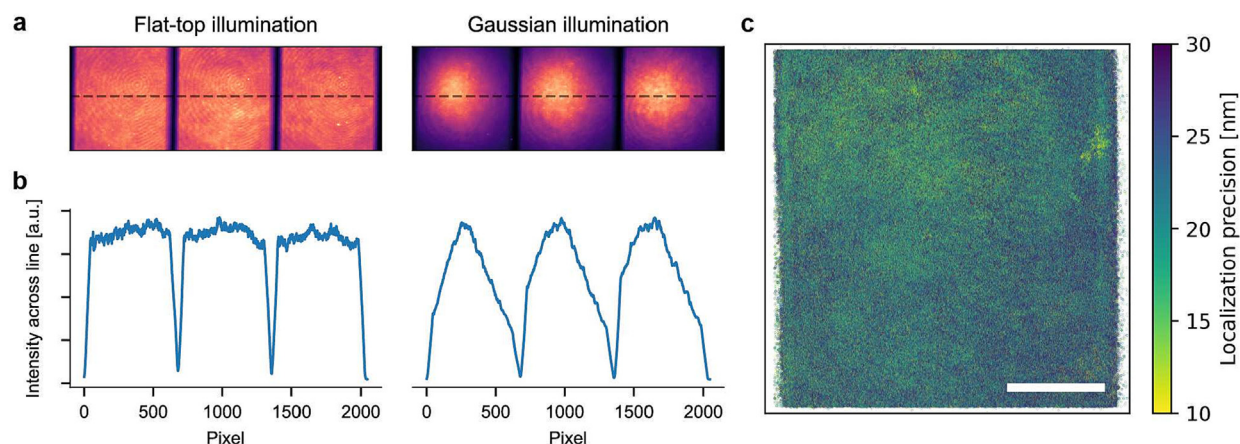
Fig. 13. Triple-color TIRF imaging of a multicolor fluorescently labeled bilayer, excited by a spatially homogeneous excitation field (**a**) versus a Gaussian beam (**b**). Laser intensities were adjusted for each color channel to produce similar peak intensities. Fields of view per color channel are 682x682 pixels, or 73.656µm x 73.656µm. **c)** Localization precision map computed from a total of 3,300,599 individual localizations of freely diffusing Cy3B-labeled reconstituted proteins on a supported lipid bilayer. The homogeneous excitation field allows precise localization of single-molecules across the entire field-of-view. Scale bar: 20µm.

the sample. This is because the lack of vignetting at the edges of the field of view allows the individual images to be easily combined into a single, large image without loss of quality (see Fig. S54, $250µm \times 250µm$ field of view). Furthermore, the focus stabilization system is able to compensate for coverslip tilt and inhomogeneities that can degrade the image quality during raster-scanning. This allows us to perform fully automated raster-scanned image acquisitions, without the need for manual intervention to maintain focus (see Fig. SM3).

7.4. Localization-based super-resolution performance

The performance of our setup in localization-based super-resolution microscopy was evaluated by imaging a commercially available DNA origami nanoruler sample (Gattaquant 2x 40nm distance, $1µm^{-2}$ surface density). The results, shown in Fig. 14, show well-resolved individual DNA binding sites and confirm the 40nm distance between the binding sites. This demonstrates the capability of our setup in achieving high-resolution imaging at the nanoscale.
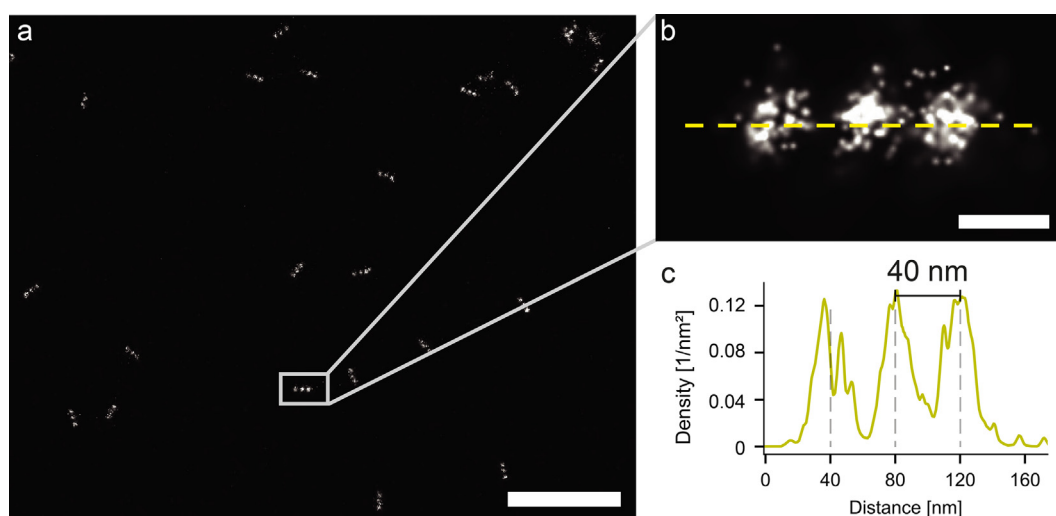

Fig. 14. DNA origami nanoruler benchmark sample. **a)** Rendered localizations of a 2 x 40nm nanoruler sample, acquired over 10,000 frames (561nm excitation wavelength, Cy3B imager strands). Scalebar: 500nm. **b)** Detailed view of one DNA origami nanoruler, with three docking sites distinctly visible. Scalebar: 40nm. **c)** Line profile of the localization density of the nanoruler shown in b), confirming the 40nm distance between DNA binding sites on the DNA origami nanoruler.

7.5. Temperature stability and objective heating response time

We use an objective heater to maintain a stable, physiological temperature of the sample during extended live-cell imaging at 37°C. The heater is controlled by a feedback loop that uses a temperature sensor at the objective to control the flow of current through a polyimide heater wrapped around the objective. Thermal decoupling of the objective and a plexiglass enclosure around the central cube help to maintain a constant temperature. The offset of objective temperature and the temperature directly at the sample was determined using a second sensor immersed in a test sample. At room temperature (21°C), the system stabilizes at an objective temperature of 42 ± 0.1°C (corresponding to 37°C at the sample) after about 20min (Fig. 15). Since there is no active cooling, it takes about 200min for the system to return to room temperature. The thermal isolation and the mass of the central cube ensure minimal heating of the rest of the setup, which is important for maintaining alignment. In fact, the environmental sensor on the central cube showed an increase in temperature of less than 1°C when the objective was heated to 42°C (Fig. S53). Overall, the objective heater is an effective and low-cost solution for maintaining a stable, physiological temperature of the sample during live-cell imaging.

7.6. Experimental applications: from live-cell imaging to single-molecule tracking

The K2 TIRF microscope can be used for a wide range of live-cell and single-molecule experiments [45]. Fig. 16 showcases several such applications: dual-color single-molecule tracking of membrane proteins on live cells, with the third channel being used for detecting a transfection reporter (1) and dual-color single-molecule tracking of reconstituted membrane proteins transiently forming dimers on a supported lipid bilayer (2), as well as localization-based super-resolution microscopy like DNA-PAINT, demonstrated here by resolving a 2x 40nm DNA origami nanoruler (3). Further applications are timelapse imaging of immune cell activation (4) and epifluorescence imaging of giant unilamellar vesicles (5), alongside brightfield imaging of an immune cell using the circular LED array. Combining epifluorescence imaging together with the z-stack function allows to capture 3D volumes of cells in suspension (6). The K2 TIRF microscope is also capable of performing fluorescence recovery after photobleaching (FRAP) experiments, here shown on a COS7 cell labeled with a fluorescent membrane marker (7).

In summary, the K2 TIRF microscope is a versatile instrument that allows the study of cellular and molecular dynamics in up to three fluorescence channels with an additional brightfield option. A large and homogeneously illuminated field-of-view, automated sample positioning and raster-scanning options enable the acquisition of high-quality, high-throughput microscopy data with comparatively little demand on user input. Furthermore, imaging experiments can be performed for extended durations (hours) due to the setup's excellent stability, active focus stabilization and objective heating for live-cell compatibility. The extensive open-source documentation should allow researchers to easily recreate the setup, or parts of it, and adapt it to their specific requirements.

Current applications of the setup:

- (Single-molecule) TIRF microscopy with simultaneous detection of up to three colors
- Experiments with environmental control (temperature) or monitoring (temperature, humidity, sample drift)
- Video-rate recording with camera-triggered excitation (alternating or continuous)
- Timelapse- and tiled acquisitions with focus stabilization
- LED-based brightfield imaging
- Widefield epifluorescence imaging
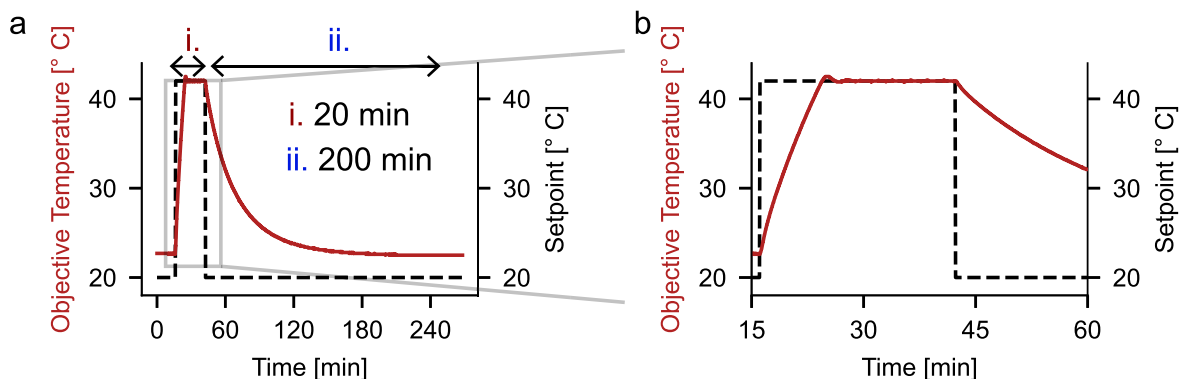- Fluorescence recovery after photobleaching (FRAP) experiments

Fig. 15. a) Heating phase, stabilized temperature and cooling phase during an objective heating cycle with a setpoint temperature of 42°C, corresponding to 37°C sample temperature. **b)** Close-up showing stabilized temperature about 20min after activating the objective heating.
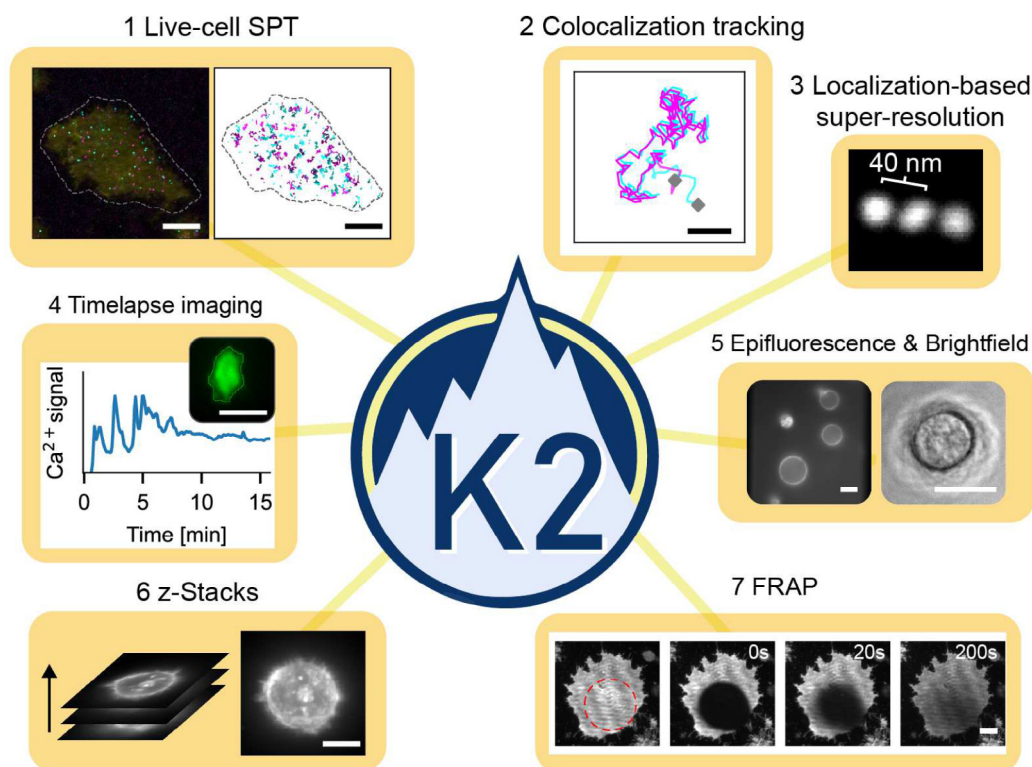
Fig. 16. Examples ofs the experiments that can be performed with the K2: (1) Dual-color single particle tracking on live Jurkat T-cells with a third channel used as a transfection reporter and (2) dual-color single-molecule tracking of reconstituted proteins on a supported lipid bilayer. Tracking the movement of two (or more) different fluorescently labeled molecules provides information about the interactions between different molecules by colocalization analysis. (3) Localization-based super-resolution microscopy, as demonstrated here by resolving a 2x 40nm DNA origami nanoruler (structures averaged using Picasso Average [42]). (4) Live-cell timelapse imaging to measure immune cell activation: Jurkat T-cell outlines are tracked using cellpose [43] and TrackMate [44] and the mean intensity of the cell-permeable green fluorescent Ca^{2+} reporter Fluo4 is measured. (5) Epifluorescence imaging of giant unilamellar vesicles (left) and brightfield imaging of an adherent Jurkat T-cell (right). (6) Maximum projection of a *z*-stack of a Jurkat T-cell in suspension, imaged in epifluorescence mode. (7) Timeseries of a fluorescence recovery after photobleaching measurements on a COS7 fibroblast cell: A reference image before the photobleaching step (left), directly after a bleaching pulse in the red circle (0s, and the subsequent recovery after 20s and 200s, showing the mobility of the fluorescently labeled membrane. All scale bars: 10μm.

Not performed currently but possible:

- Single-molecule Förster resonance energy transfer (FRET) microscopy
- Multi-color super-resolution microscopy: DNA-PAINT, Photo-activated localization microscopy (PALM), stochastic optical reconstruction microscopy (STORM)

Funding

Declaration of Competing Interest

The authors declare that they have no known competing financial interests or personal relationships that could have appeared to influence the work reported in this paper.

Acknowledgement

Appendix A. Supplementary data

Supplementary data associated with this article can be found, in the online version, at https://doi.org/10.1016/j.ohx.2023.e00404.

References

[1] Hongqiang Ma et al. A Simple and Cost-Effective Setup for Super-Resolution Localization Microscopy. In: Scientific Reports 7.1 (2017). doi: 10.1038/s41598-017-01606-6.

[2] Alexander Auer et al, Nanometer-Scale Multiplexed Super-Resolution Imaging with an Economic 3DDNA-PAINT Microscope, ChemPhysChem (2018), https://doi.org/10.1002/cphc.201800630.

[3] Koen J. A. Martens et al. Visualisation of dCas9 Target Search in Vivo Using an Open-Microscopy Framework. In: Nature Communications 10.1 (2019), p. 3552. doi: 10.1038/s41467-019-11514-0.

[4] Benedict Diederich et al. A Versatile and Customizable Low-Cost 3D-printed Open Standard for Microscopic Imaging. In: Nature Communications 11.1 (1 2020), p. 5979. doi: 10.1038/s41467-020-19447-9.

[5] Mohammad Nour Alsamsam et al. The miEye: Bench-top Super-Resolution Microscope with Cost- Effective Equipment. In: HardwareX 12 (2022), e00368. doi: 10.1016/j.ohx.2022.e00368.

[6] John S.H. Danial et al, Constructing a Cost-Efficient, High-Throughput and High-Quality Single-Molecule Localization Microscope for Super-Resolution Imaging, Nature Protocols (2022), https://doi.org/10.1038/s41596-022-00730-6.

[7] Johannes Hohlbein et al. Open Microscopy in the Life Sciences: Quo Vadis? In: Nature Methods 19.9 (2022), pp. 1020–1025. doi: 10.1038/s41592-022-01602-3.

[8] Mad City Labs. TIRF Lock- Keeps the Sample in the Focal Plane and Maintains TIRF Signal. 2022. url: http://www.madcitylabs.com/tirf-lock.html (visited on 12/20/2022).

[9] ASI Imaging. CRISP Autofocus System. 2022. url: https://www.asiimaging.com/products/focus-controland-stabilization/crisp-autofocus-system/ (visited on 12/20/2022).

[10] Karl Bellve et al, Design and Implementation of 3D Focus Stabilization for Fluorescence Microscopy, Biophysical Journal 106 (2) (2014) 606a.

[11] Daniel Schröder et al. Cost-Efficient Open Source Laser Engine for Microscopy. In: Biomedical Optics Express 11.2 (2020), p. 609. doi: 10.1364/BOE.380815.

[12] Jeff Y.L. Lam et al, An Economic, Square-Shaped Flat-Field Illumination Module for TIRF-based Super-Resolution Microscopy, Biophysical Reports 2 (1) (2022), https://doi.org/10.1016/j.bpr.2022.100044 100044.

[13] Andor. Microscope Light Source - Integrated Laser Engine - ILE. Oxford Instruments. 2022. url: https://www.andor.oxinst.com/products/microscopy-components/integrated-laser-engine (visited on 12/20/2022).

[14] John Philippi and Johannes Hohlbein. SMILE: Single Molecule Imaging Laser Engine. SMILE: SingleMolecule Imaging Laser Engine. 2022. url: https://hohlbeinlab.github.io/miCube/LaserTrack Arduino. html (visited on 12/20/2022).

[15] Mohammed Mahamdeh, Erik Schäffer, Optical Tweezers with Millikelvin Precision of Temperature- Controlled Objectives and Base-Pair Resolution, Optics Express 17 (19) (2009) 17190, https://doi.org/10.1364/OE.17.017190.

[16] Andy Maloney, Lawrence J. Herskowitz, Steven J. Koch, Effects of Surface Passivation on Gliding Motility Assays, PLOS ONE 6 (6) (2011), https://doi.org/10.1371/journal.pone.0019522 e19522.

[17] Khalid A. Ibrahim, Dora Mahecic, Suliana Manley, Characterization of Flat-Fielding Systems for Quantitative Microscopy, Optics Express 28 (15) (2020) 22036, https://doi.org/10.1364/OE.395900.

[18] Ian Khaw et al, Flat-Field Illumination for Quantitative Fluorescence Imaging, Optics Express 26 (12) (2018) 15276, https://doi.org/10.1364/OE.26.015276.

[19] Florian Stehr et al. Flat-Top TIRF Illumination Boosts DNA-PAINT Imaging and Quantification. In: Nature Communications 10.1 (2019), p. 1268. doi: 10.1038/s41467-019-09064-6.

[20] Paula Montero Llopis et al. Best Practices and Tools for Reporting Reproducible Fluorescence Microscopy Methods. In: Nature Methods 18.12 (2021), pp. 1463–1476. doi: 10.1038/s41592-021-01156-w.

[21] Bioptechs. Objective Heater - Bioptechs. 2022. url: https://bioptechs.com/product/objective-heater/(visited on 12/20/2022).

[22] Philip R. Nicovich et al. NicoLase-An Open-Source Diode Laser Combiner, Fiber Launch, and Sequencing Controller for Fluorescence Microscopy. In: PLOS ONE 12.3 (2017), e0173879. doi: 10.1371/journal. pone.0173879.

[23] CAIRN Research. Triggerscope 4 - Core And Analysis - Cairn Research Ltd. Cairn Research. 2022. url: https://www.cairn-research.co.uk/product/triggerscope-4/ (visited on 12/20/2022).

[24] Teledyne. OptoSplit III - Teledyne Photometrics. 2022. url: https://www.photometrics.com/products/imaging-splitters/optosplit-iii (visited on 12/20/2022).

[25] Simao Coelho et al. 3D Active Stabilization for Single-Molecule Imaging. In: Nature Protocols 16.1 (2021), pp. 497–515. doi: 10.1038/s41596-020-00426-9.

[26] Michael J. Saxton, Ken Jacobson, Single-particle tracking: Applications to Membrane Dynamics, Annual Review of Biophysics and Biomolecular Structure 26 (1) (1997) 373–399, https://doi.org/10.1146/annurev.biophys.26.1.373.

[27] Laura Marchetti et al. Ligand Signature in the Membrane Dynamics of Single TrkA Receptor Molecules. In: Journal of Cell Science 126.19 (2013), pp. 4445–4456. doi: 10.1242/jcs.129916.

[28] Alex J. B. Kreutzberger et al. Rhomboid Distorts Lipids to Break the Viscosity-Imposed Speed Limit of Membrane Diffusion. In: Science 363.6426 (2019), eaao0076. doi: 10.1126/science.aao0076.

[29] Andres I. König et al. Live Cell Single Molecule Tracking and Localization Microscopy of Bioorthogonally Labeled Plasma Membrane Proteins. In: Nanoscale 12.5 (2020), pp. 3236–3248. doi: 10.1039/C9NR08594G.

[30] Benedict Diederich et al, CAD We Share? Publishing Reproducible Microscope Hardware, Nature Methods 19.9 (9 2022) 1026–1030, https://doi.org/10.1038/s41592-022-01484-5.

[31] Sara Abrahamsson et al, MultiFocus Polarization Microscope (MF-PolScope) for 3D Polarization Imaging of up to 25 Focal Planes Simultaneously, Optics Express 23 (6) (2015) 7734, https://doi.org/10.1364/OE.23.007734.

[32] Rainer Heintzmann. Practical Guide to Optical Alignment. In: Fluorescence Microscopy. Ed. by Ulrich Kubitscheck. Weinheim, Germany: Wiley-VCH Verlag GmbH & Co. KGaA, 2017, pp. 463–471. doi: 10.1002/9783527687732.app2.

[33] Arthur Edelstein et al. Computer Control of Microscopes Using Manager. In: Current Protocols in Molecular Biology 92.1 (2010). doi: 10.1002/0471142727.mb1420s92.

[34] A. L. Mattheyses, S. M. Simon, and J. Z. Rappoport. Imaging with Total Internal Reflection Fluorescence Microscopy for the Cell Biologist. In: Journal of Cell Science 123.21 (2010), pp. 3621–3628. doi: 10.1242/jcs.056218.

[35] Junel Sotolongo Bellón et al. Four-Color Single-Molecule Imaging with Engineered Tags Resolves the Molecular Architecture of Signaling Complexes in the Plasma Membrane. In: Cell Reports Methods 2.2 (2022), p. 100165. doi: 10.1016/j.crmeth.2022.100165.

[36] Kaley A. McCluskey et al, Global Correction of Optical Distortions in Multicolor Single-Molecule Microscopy Using Zernike Polynomial Gradients, Optics Express 29 (25) (2021) 42251, https://doi.org/10.1364/OE.445230.

[37] Sang Hak Lee et al, Using Fixed Fiduciary Markers for Stage Drift Correction, Optics Express 20 (11) (2012) 12177, https://doi.org/10.1364/OE.20.012177.

[38] Ryan McGorty, Daichi Kamiyama, Bo Huang, Active Microscope Stabilization in Three Dimensions Using Image Correlation, Optical Nanoscopy 2 (1) (2013) 3, https://doi.org/10.1186/2192-2853-2-3.

[39] Yeoan Youn et al, Thermal Nanoimprint Lithography for Drift Correction in Super-Resolution Fluorescence Microscopy, Optics Express 26 (2) (2018) 1670, https://doi.org/10.1364/OE.26.001670.

[40] Smaract. Stick-Slip Drive Technology. 2022. url: https://www.smaract.com/en/technology-introductionand-options#position-sensors (visited on 12/20/2022).

[41] ASI. MS-2000 XYZ Automated Stage. 2022. url: https://www.asiimaging.com/downloads/datasheets/MS-2000XY-Datasheet-Web.pdf (visited on 12/20/2022).

[42] Joerg Schnitzbauer et al. Super-Resolution Microscopy with DNA-PAINT. In: Nature Protocols 12.6 (2017), pp. 1198–1228. doi: 10.1038/nprot.2017.024.

[43] Carsen Stringer et al. Cellpose: A Generalist Algorithm for Cellular Segmentation. In: Nature Methods 18.1 (2021), pp. 100–106. doi: 10.1038/s41592-020-01018-x.

[44] Dmitry Ershov et al. TrackMate 7: Integrating State-of-the-Art Segmentation Algorithms into Tracking Pipelines. In: Nature Methods 19.7 (2022), pp. 829–832. doi: 10.1038/s41592-022-01507-1.

[45] Christian Niederauer et al. DNA-PAINT Single-Particle Tracking (DNA-PAINT-SPT) Enables Extended Single-Molecule Studies of Membrane Protein Interactions. In: bioRxiv (2022), p. 2022.08.25.503948. doi: 10.1101/2022.08.25.503948.

Christian Niederauer received B.S. and M.S. degrees in Physics from the Ludwig-Maximilians University in Munich, Germany, during which he had the opportunity to study abroad at IISER Pune in India, and Boğaziç?i University in Istanbul, Turkey. Currently, he is pursuing his PhD at the Institute for Atomic and Molecular Physics (AMOLF) in Amsterdam, The Netherlands. His research interests include single-molecule biophysics, fluorescence microscopy and scientific technology development.

Kristina A. Ganzinger received her PhD in Physical Chemistry from the University of Cambridge (UK) in 2015, under the guidance of Sir Prof. David Klenerman. After a postdoc at the Max Planck Institute for Biochemistry (GER) with Prof. Petra Schwille, she began her current position as tenure-track group leader at the NWO physics institute AMOLF (NL) in 2018. The central questions driving her research are: How do cells transmit, process and respond to information, both precisely and unambiguously, and how do they shape their membranes in response? And if we understand the molecular mechanisms of cell signalling, can we design and tune artificial (protein-based) signalling networks? Her lab's approach is to address these questions by (1) in vitro reconstitution in model-membrane systems ("minimal cells") and (2) pairing these studies with live-cell experiments. They use custom microscopy, quantitative data analysis and, in collaboration, predictive mathematical modelling to understand the underlying molecular mechanisms, and for this continuously develop new (single-molecule) microscopy methods. Her group is passionate about open access science and sharing methods via Github and Pre-prints.